

# Critical exponents for the Ising model between one and two dimensions

M. A. Novotny

*Supercomputer Computations Research Institute B-186, Florida State University,  
Tallahassee, Florida 32306-4052*

(Received 10 October 91; revised manuscript received 16 January 1992)

Critical exponents are presented for the ferromagnetic Ising model in dimensions between one and two. The exponents are calculated by applying finite-size-scaling methods to numerical transfer-matrix data. The transfer matrix, which is translationally invariant, is written in such a fashion that interpolation to noninteger dimensions is possible. Results are also obtained for the first derivatives evaluated at  $d=2$  for the critical exponents  $\nu_T$  and  $\nu_H$  as a function of dimension. All results are compared with series-expansion results in  $1 < d \leq 2$ .

## I. INTRODUCTION

Our current understanding of critical behavior, particularly critical exponents, associated with classical statistical-mechanical models has benefited significantly from the use of the concept of variable dimensions. Various theoretical methods of performing expansions in the dimension,  $d$ , have been devised. These include series expansions for high-dimensional systems,<sup>1-3</sup> the Wilson-Fisher expansion in  $d = 4 - \epsilon$  dimensions,<sup>4-9</sup> expansions in  $d = 1 + \epsilon$  for the near-planar interface<sup>10-12</sup> and for the droplet<sup>13</sup> models, the Kadanoff variational renormalization-group (RG) method,<sup>14-16</sup> and the Migdal-Kadanoff bond-shifting technique.<sup>16-18</sup>

Similar techniques for continuous values of  $d$  have been instrumental in understanding a wide variety of systems, including the critical behavior of disordered systems,<sup>19,20</sup> the  $O(n)$  Heisenberg model,<sup>21</sup> the  $q$ -state Potts model,<sup>16</sup> self-avoiding walks,<sup>22</sup> random resistor networks,<sup>23</sup> and fluctuations of solid membranes.<sup>24</sup>

The Migdal-Kadanoff<sup>17,18</sup> bond-shifting technique, which provides approximate results on Bravais lattices, has been shown to be the exact solution of hierarchical models.<sup>25,26</sup> It had been suggested that hierarchical lattices and other fractal lattices<sup>27,28</sup> could lead to critical exponents which would interpolate the results on regular lattices to noninteger dimensions. For example, the critical exponent  $\nu$  associated with the divergence of the correlation length at the critical temperature should have some functional dependence on only the dimension,  $\nu = \nu(d)$ . Consequently model Hamiltonians, such as the Ising-model Hamiltonian, have been studied using real-space renormalization-group methods,<sup>29-32</sup> Monte Carlo methods,<sup>33,34</sup> and series expansions.<sup>35,36</sup> It has been shown that these systems belong to universality classes which are governed not only by the Hausdorff (fractal) dimension,  $d$ , but also by other parameters, such as ramification, connectivity, and lacunarity. Although Ising spin systems on fractals with infinite ramification have a nonzero critical temperature,<sup>37</sup> even for these fractal lattices the universality class depends on other parameters.<sup>29,31,34,35,37-40</sup> Only in the limit where translational invariance is recovered, the limit where the

lacunarity approaches zero, is it now believed that Ising systems on fractal lattices may interpolate hypercubic-lattice results.<sup>9,29,31,34,35</sup> Unfortunately, this is a limit where nonperturbative numerical calculations are difficult to perform.<sup>31</sup> Since critical exponents such as  $\nu$  for the short-ranged ferromagnetic Ising model should be only a function of the dimension  $d$ , one should seek an alternative to studies on fractal lattices to test series-expansion results in  $d$ .

In this paper an alternative method is presented that interpolates continuously between integer dimensions, and that preserves translational symmetry. This interpolation method is extremely compatible with the numerical transfer-matrix method, and this method of study is used in the present paper. Although the interpolation method should be applicable to any classical statistical-mechanical lattice model, only results for the ferromagnetic Ising model on hypercubic lattices will be presented here. Preliminary results for this interpolation scheme have previously been published.<sup>41-44</sup> The interpolation scheme is also related to a method of studying the Ising model in high dimensions using numerical transfer-matrix results.<sup>45-47</sup>

Once the interpolation scheme is introduced, it is assumed that finite-size scaling of transfer-matrix data still holds for the interpolated transfer matrix. This assumption then gives finite-size estimates for the dimension of the system and the critical exponents for the system. The interpolation method presented here is only one possible method of obtaining critical exponents and has many weaknesses. As will be seen in Sec. III, critical exponents are obtained which agree extremely well with results from series expansions. However, nonuniversal quantities, such as the critical temperature, obtained with this method suffer from pathologies related to whether or not the thermodynamic limit exists in the interpolation scheme. Part of the question regarding the existence of the thermodynamic limit of the interpolation scheme comes from using finite-size scaling to obtain the dimension as a function of the interpolation parameter.

Section II presents the model, a compilation of previous results by other techniques, the interpolation method, and the finite-size-scaling method used on the

numerical data. Section III contains the data and comparisons with other results. Section IV contains the results and conclusions.

## II. MODEL AND METHOD

The Ising model has a Hamiltonian given by

$$\mathcal{H} = -J \sum_{\langle i,j \rangle} s_i s_j - H \sum_i s_i, \quad (1)$$

where the spins  $s_i = \pm 1$ , and the summation is over nearest-neighbor sites on a lattice. Here  $H$  is the magnetic field and  $J$  is the two-body coupling constant.

For  $1 < d$  the Ising model has a phase transition at a finite critical temperature,  $T_c$ . At  $T_c$  the largest thermal exponent is  $y_T = 1/\nu$  and the largest magnetic exponent is  $y_H$ . Other critical exponents can be determined from scaling and hyperscaling formulas as demonstrated in Sec. III. The critical exponents for translationally invariant, ferromagnetic, short-range interactions depend *only* on the dimension of the lattice.

### A. Previous results for $1 < d < 2$

Since it will be necessary to compare the numerical results obtained below with other results for the Ising model in  $1 \leq d \leq 2$ , this section collects the relevant results. Table I summarizes results for the critical exponents  $y_T$  and  $y_H$  from Wilson-Fisher expansions in  $d = 4 - \epsilon$  which were resummed to include the exact result at  $d = 2$ .<sup>9</sup> This is condensed from Table III of Ref. 9, with  $\eta = d + 2 - 2y_H$ . The exact values for  $d = 2$  are shown in the appropriate columns. Table I also includes recent results from a variational method derived from high-temperature series expansions.<sup>48</sup> The results are from Table II of Ref. 48. The error bounds for  $y_H$  are chosen to include all of the published results.

We will also compare our numerical results with expansions in  $d = 1 + \epsilon$  for the near-planar interface model of Wallace and Zia. The result for  $y_T = 1/\nu$  is given by the asymptotic expansion in  $\epsilon = d - 1$  as<sup>10-12</sup>

$$\nu = \frac{1}{\epsilon} - \frac{1}{2} + \frac{\epsilon}{2} - \frac{7\epsilon^2}{8} + O(\epsilon^3). \quad (2)$$

This asymptotic series happens to go through the exact value  $\nu = 1$  at  $d = 2$  if the series is truncated after either

the first (one-loop) or the third (three-loop) term.

A further extension of this model, the droplet model,<sup>13</sup> gives the critical exponent

$$d - y_H = 4\pi^{-1} \epsilon^{-(2+\epsilon)/2} \exp\left\{-[1+2C+(2/\epsilon)]\right\} [1+O(\epsilon)], \quad (3)$$

where  $C = 0.577 \dots$  is Euler's constant. Whether or not these models correspond to the Ising model in arbitrary dimension has been questioned. In particular, the near-planar interface model ignores bubbles and overhangs, which are relevant operators near  $T_c$ .<sup>49</sup> Nevertheless, it has been shown<sup>13,50</sup> that such corrections vanish as an essential singularity for  $d \rightarrow 1$ , and that the isotropic fixed point is stable to a wide class of perturbations,<sup>51</sup> so the  $d = 1 + \epsilon$  expansion of the near-planar interface model may be formally correct.

### B. Transfer-matrix method for $1 < d \leq 2$

Consider a nearest-neighbor Ising model on a  $d$ -dimensional hypercubic lattice. Let the system be composed of  $N$  Ising spins in each  $(d-1)$ -dimensional layer, with  $M$  identical layers. Number the layers so layer  $i$  interacts only with layers  $i-1$  and  $i+1$ . The partition function then can be written as<sup>52-55</sup>

$$Z = \text{Tr}[(\underline{D}_H \underline{D}_{d-1} \underline{A})^M]. \quad (4)$$

The matrix  $\underline{D}_{d-1}$  contains all interactions between the spins within a  $(d-1)$ -dimensional layer. Hence, all of the information about the dimension is contained in the  $2^N \times 2^N$  matrix  $\underline{D}_{d-1}$ , which can be chosen to be a diagonal matrix. The matrix  $\underline{A}$  is a direct (Kronecker) product of  $N$  identical  $2 \times 2$  matrices

$$\underline{a} = \begin{pmatrix} e^K & e^{-K} \\ e^{-K} & e^K \end{pmatrix}, \quad (5)$$

where  $K = J/k_B T$  with  $J$  the nearest-neighbor interaction constant,  $k_B$  Boltzmann's constant, and  $T$  the temperature. The matrix  $\underline{A}$  connects each layer with the subsequent layer, and is independent of the interactions within a  $(d-1)$ -dimensional layer, and is given by  $\underline{A} = \underline{a} \otimes \underline{a} \otimes \dots \otimes \underline{a}$  where  $\otimes$  denotes the Kronecker matrix product and there are  $N$   $\underline{a}$  matrices in the product. The diagonal matrix  $\underline{D}_H$  contains interactions between

TABLE I. The thermal and magnetic critical exponents from series expansions are shown. See the text for a full description.

$d$	From Ref. 9		From Ref. 48	
	$y_T$	$y_H$	$y_T$	$y_H$
2.0	1.0	1.875	0.9862-1.0091	1.8735-1.8765
1.875	0.9009-0.9174	1.7765-1.8025	0.8850-0.9009	1.7725-1.7815
1.75	0.7937-0.8333	1.6750-1.7250	0.7937-0.8475	1.6625-1.6770
1.65	0.6944-0.7692	1.5750-1.6750	0.7246-0.7874	1.5715-1.6000
1.5	0.5405-0.6897	1.4250-1.5750	0.5435-0.6711	1.4345-1.4665
1.375	0.3846-0.6250	1.2875-1.5375	0.3448-0.6250	1.3480-1.3700
1.25	0.2222-0.6667	1.1250-1.4750	0.2941-0.5882	1.2100-1.2460

the spins and an external magnetic field, and is given by the Kronecker product of  $N$  matrices

$$\underline{h} = \begin{pmatrix} e^{H/k_B T} & 0 \\ 0 & e^{-H/k_B T} \end{pmatrix}. \quad (6)$$

Now assume helical boundary conditions in the  $(d-1)$ -dimensional hypercubes. Then a form for the diagonal matrix which can interpolate continuously between one and two dimensions can be written as<sup>41</sup>

$$\underline{D}_v = \underline{I} \odot (\underline{P}^v \underline{A}). \quad (7)$$

Here  $\odot$  stands for Hadamard (element by element) matrix multiplication, and  $\underline{I}$  is the  $2^N \times 2^N$  identity matrix. The permutation matrix  $\underline{P}$  is the matrix such that  $\underline{P}^{-1} \underline{A} \underline{P}$  permutes the  $2 \times 2$  matrices  $\underline{a}$  of Eq. (5) within the Kronecker product in a cyclic fashion,  $1 \rightarrow 2 \rightarrow \dots \rightarrow N \rightarrow 1$ .<sup>41,55,56</sup> Thus

$$\begin{aligned} \underline{P}^{-1}(\underline{a}_1 \otimes \underline{a}_2 \otimes \underline{a}_3 \otimes \dots \otimes \underline{a}_{N-1} \otimes \underline{a}_N) \underline{P} \\ = \underline{a}_N \otimes \underline{a}_1 \otimes \underline{a}_2 \otimes \dots \otimes \underline{a}_{N-2} \otimes \underline{a}_{N-1}. \end{aligned} \quad (8)$$

Equation (7) gives the diagonal matrix by simply taking the diagonal elements of the matrix  $\underline{A}$  multiplied by the permutation matrix  $\underline{P}$  raised to the power  $v$ . If  $v$  is an integer, the diagonal elements in Eq. (7) simply give the interaction between spins at lattice site  $i$  and  $i+v$  (with periodic boundary conditions), and hence describe the connectivity of the lattice.

When  $v = 1$ , the diagonal matrix  $\underline{D}_v$  is identical to the diagonal matrix  $\underline{D}_1$  for the  $d = 2$  Ising model on a square lattice.<sup>54</sup> When  $v = 0$  the diagonal matrix is  $\underline{D}_0 = \underline{I} \exp(NK)$ , so the system describes  $N$  uncoupled one-dimensional Ising chains. Thus, the parameter  $v$  can be used to try to interpolate continuously between one and two dimensions. Note that the value of  $J$  is not changed in this interpolation, rather the interpolation scheme changes the connectivity, since it acts only on the permutation matrix  $\underline{P}$ . Also, it is clear that the system has translational invariance, since both  $\underline{D}_v$  and  $\underline{A}$  commute with  $\underline{P}$ , the generator of single-step translations in the finite direction.

One difficulty which is inherent in Eq. (7) is that the reflection symmetry,  $(1, 2, \dots, N-1, N) \leftrightarrow (N, N-1, \dots, 2, 1)$ , is not preserved when  $v$  is not an integer. This is remedied by using the diagonal matrix given by

$$\bar{\underline{D}}_v = \underline{I} \odot (\underline{P}^v \bar{\underline{A}}) \odot (\underline{P}^{-v} \bar{\underline{A}}), \quad (9)$$

where  $\bar{\underline{A}}$  is the same as the Kronecker-product matrix  $\underline{A}$  except that it has an interaction constant  $J/2$  rather than  $J$  in the matrix given by Eq. (5).

We now detail how the diagonal matrix is constructed for  $v$  values which are not in general an integer. The power of the matrix is given by

$$\underline{P}^v = \sum_{k=1}^{2^N} |k\rangle p_k^v \langle k|, \quad (10)$$

where  $|k\rangle$  is the eigenvector of  $\underline{P}$  associated with eigen-

value  $p_k$ . The eigenvalues of  $\underline{P}$  are the  $N$  roots of unity,  $p_k = \exp(i\phi_k)$ . The eigenvectors  $|k\rangle$  can be formed from the eigenvectors of the matrix  $\underline{A}$ . These are Kronecker products of the two orthonormal eigenvectors  $|u_+\rangle$  and  $|u_-\rangle$  associated with the eigenvalues  $\kappa_{\pm} = \exp(K) \pm \exp(-K)$  of the matrix  $\underline{a}$  in Eq. (5). A normalized eigenvector  $|k\rangle$  of  $\underline{A}$  with eigenvalue  $\Phi_k = \kappa_+^m \kappa_-^{N-m}$  with  $0 \leq m \leq N$  and eigenvalue  $p_k$  of  $\underline{P}$  is then constructed by

$$|k\rangle = E_k^{-1/2} \sum_{\ell=1}^{E_k} p_k^{\ell} \underline{P}^{\ell} |U_m\rangle. \quad (11)$$

Here  $|U_m\rangle$  is the eigenvector of  $\underline{A}$  formed by a Kronecker product of  $m$  vectors  $|u_+\rangle$  and  $N-m$  vectors  $|u_-\rangle$  in some particular order. The sum in Eq. (11) is over all  $E_k$  distinct permutations of the vectors formed by multiplying by some integer power of  $\underline{P}$  ( $E_k \leq N$ , and  $E_k = N$  whenever  $N$  is a prime number). Performing this procedure with all inequivalent combinations of the vectors formed from Kronecker products of  $|u_+\rangle$  and  $|u_-\rangle$  gives a complete set of orthonormal eigenvectors of  $\underline{A}$  and  $\underline{P}$ .

Let  $|S\rangle$  be the physical state with a particular choice of the Ising spins  $s_j = \pm 1$ . Then from Eqs. (7) and (10) the elements of the diagonal matrix are formed from the eigenvectors constructed in Eq. (11) by

$$\langle S | \underline{D}_v | S \rangle = \sum_{k=1}^{2^N} \exp(iv\phi_k) \langle S | k \rangle \langle k | \underline{A} | S \rangle. \quad (12)$$

However  $\langle k|$ , the Hermitian conjugate of  $|k\rangle$ , is also an eigenvector of  $\underline{A}$  with eigenvalue  $\Phi_k$ , so this can be rewritten as

$$\langle S | \underline{D}_v | S \rangle = \sum_{k=1}^{2^N} \exp(iv\phi_k) \Phi_k |\langle S | k \rangle|^2. \quad (13)$$

Thus, even though the elements of  $|k\rangle$  are complex this does not affect whether the elements of  $\underline{D}_v$  are real.

We also have the freedom to choose the phases  $\phi_k$ . For odd  $N$  we choose the values  $\phi_k = \frac{2\pi k}{N}$  with  $k = 0, \pm 1, \dots, \pm \frac{N-1}{2}$ . Then all the elements of  $\underline{D}_v$  in Eq. (13) are real and positive. This is because the phases enter as complex-conjugate pairs, and each pair has the same value for  $\Phi_k$  and the same values for  $|\langle S | k \rangle|^2$  since they were formed by the prescription in Eq. (11). Thus when  $N$  is odd all the elements of  $\underline{D}_v$  are positive. For even  $N$  the root of unity  $\phi_k = \pi$  does not allow for a simple pairing method to make the elements of  $\underline{D}_v$  real. Consequently, we will henceforth restrict ourselves to odd values of  $N$ .

### C. Finite-size-scaling method

The correlation length for an  $N \times \infty$  Ising model is given by the ratio of the largest and next-largest eigenvalue of the transfer matrix  $\underline{D}_H \underline{D}_v \underline{A}$  as  $\xi(T, N) = 1/\ln|\Lambda_0/\Lambda_1|$ . Provided that the model is between the upper and lower critical dimension ( $1 < d < 4$  for the Ising

model), near  $H = 0$  and  $T = T_c$  of a second-order transition the correlation length should asymptotically scale as<sup>57</sup>

$$\xi(T, H, N) = N^{1/(d-1)} \mathcal{F}\left(tN^{y_T/(d-1)}, HN^{y_H/(d-1)}\right), \quad (14)$$

where  $t = |1 - T/T_c|$ .

One disadvantage of the interpolation procedure described in Sec. II B is that if  $\nu$  is not an integer, the function  $d(\nu)$  is not known. Nevertheless, by using modified finite-size scaling of numerical transfer-matrix data the dimension can be obtained. At  $H = 0$  define

$$\Omega_{ij}(T) = \ln[\xi(T, N_i)/\xi(T, N_j)]/\ln(N_i/N_j). \quad (15)$$

If  $T_c$  were known exactly,  $\Omega_{ij}(T_c)$  could be viewed as the phenomenological-renormalization<sup>58</sup> finite-size estimate of  $1/(d-1)$ . By using three lattice sizes and locating the minimum of the function  $R(T)$  defined by

$$R(T)^2 = (\Omega_{12} - \Omega_{13})^2 + (\Omega_{12} - \Omega_{23})^2 + (\Omega_{13} - \Omega_{23})^2 \quad (16)$$

with respect to  $T$ , it is possible to obtain finite-size estimates for both  $T_c$  and  $1/(d-1)$ . This possibility was mentioned in Ref. 59, but was not further investigated. An example of the function  $R(T)$  is shown in Fig. 1. For all values of  $N$  and  $\nu$  the function  $R(T)$  was found to have only a single finite-temperature minimum.

Differentiating Eq. (14) with respect to  $T$  and evaluating it at  $H = 0$  and the finite-size estimate for  $T_c$ , gives

$$\frac{y_T + 1}{d - 1} = \ln \left[ \frac{\partial \xi(T, N_i)/\partial T}{\partial \xi(T, N_j)/\partial T} \right] / \ln(N_i/N_j). \quad (17)$$

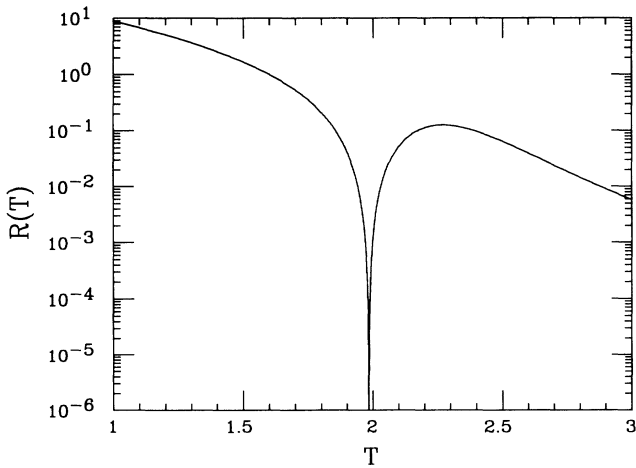


FIG. 1. The function  $R(T)$  from Eq. (16) is shown as a function of temperature. This is for the symmetric implementation with  $N = 7, 9$ , and  $11$  with  $\nu = 0.97$ . The location of the finite- $T$  minimum gives the finite-size estimate for the critical temperature,  $T_c$ . The scale of  $T$  has been chosen so  $J/k_B = 1$ .

The ratio of  $(y_T + 1)/(d - 1)$  with  $1/(d - 1)$  then gives an estimate for  $y_T$ .

In a similar fashion to Eq. (17), differentiating Eq. 14 twice with respect to  $H$ , and then evaluating it at  $H = 0$  and the finite-size estimate for  $T_c$  gives an estimate for

$$\frac{2y_H + 1}{d - 1} = \ln \left[ \frac{\partial^2 \xi(T, N_i)/\partial H^2}{\partial^2 \xi(T, N_j)/\partial H^2} \right] / \ln(N_i/N_j). \quad (18)$$

In this case the second derivative must be taken since the system is finite in all but one direction so that  $\partial \xi(T, N_i)/\partial H|_{H=0} = 0$ .

### III. DATA AND ANALYSIS

The results for critical exponents as a function of  $d$  (which will be presented below in Figs. 4–9), appear to be extremely good, and compare favorably with the  $d = 4 - \epsilon$  and  $d = 1 + \epsilon$  expansions. However, first we show the behavior of the dimension  $d$  obtained from finite-size scaling as a function of  $\nu$ . Figure 2 shows the finite-size estimates for  $d$  obtained at the fixed values of  $\nu$  for the symmetrized transfer matrix of Eq. (9). The finite-size scaling described by Eqs. (14)–(18) was performed with  $\nu$  in the interpolation scheme kept fixed for each of the three lattice sizes used for each data point. As  $N_1$  becomes larger, this function becomes closer to a step function. Consequently,  $\nu$  must not be considered to be the dimension, as was done in Ref. 41. Rather there exists some function  $d = f(\nu, N_1)$ , which may be continuous for large but finite  $N_1$ , such that  $f(0, N_1) \rightarrow 1$  and  $f(1, N_1) \rightarrow 2$  as  $N_1 \rightarrow \infty$ . Figure 2 illustrates one inherent weakness of the present method, namely the possi-

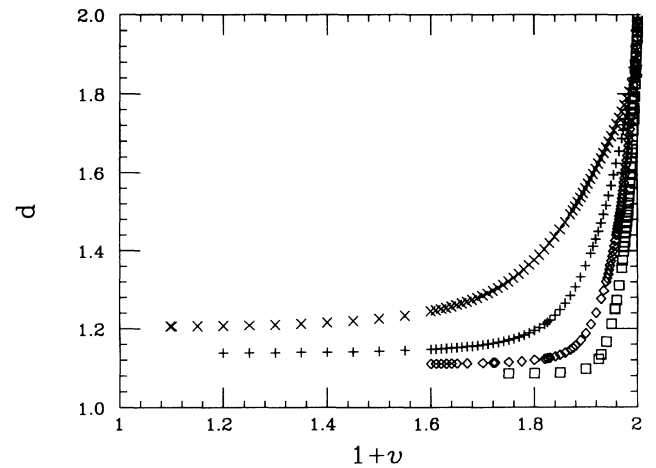


FIG. 2. The dimension  $d$  obtained from the finite-size scaling is shown as a function of the interpolation parameter  $1 + \nu$ . The symbols represent results obtained from finite-size scaling of numerical transfer-matrix data for the Ising model using three system sizes:  $\times$  for  $N = 3, 5$ , and  $7$ ;  $+$  for  $N = 5, 7$ , and  $9$ ;  $\diamond$  for  $N = 7, 9$ , and  $11$ ;  $\square$  for  $N = 9, 11$ , and  $13$ ; a fancy square for  $N = 11, 13$ , and  $15$ ; a fancy horizontal cross for  $N = 13, 15$ , and  $17$ ; and a fancy diamond for  $N = 15, 17$ , and  $19$ . For the last three symbols only a single point obtained with  $\nu = 1$  is shown.

bility that the thermodynamic limit ( $N_1 \rightarrow \infty$ ) does not exist for  $d = f(\nu, N_1)$ . If the limit does not exist, then this interpolation method of obtaining critical exponents should be viewed as a computational method. Another weakness of the method is that each curve in Fig. 2 comes from three lattice sizes, so a given lattice size  $N$  enters in three different curves in Fig. 2. Consequently there is not a single value of  $\nu$  that would give a single value of  $d$  to the lattice with strip width  $N$ .

Figure 3 shows that the critical temperature also exhibits large finite-size effects. Also shown in Fig. 3 are the results for the  $d = 1 + \epsilon$  expansion of the near-planar interface model,<sup>10-12</sup> which gives

$$k_B T_c = 2J \left( \epsilon - \frac{\epsilon^2}{2} + \frac{3\epsilon^3}{8} - \frac{7\epsilon^4}{16} + O(\epsilon^5) \right). \quad (19)$$

The  $d = 1 + \epsilon$  results for  $T_c$  do not have the same functional form as the results for  $T_c$  from our numerical transfer-matrix study. This should not be considered to be very surprising since, unlike the critical exponents,  $T_c$  is a nonuniversal quantity and may depend explicitly on the parameters of the particular model.

Data were not obtained for lower values of  $d$  than those shown due to numerical difficulties associated with underflow and overflow when the critical temperature becomes small. Figures 2 and 3 together illustrate the numerical difficulty involved in trying to reach lower values of  $d$  for a given  $N_1$ . At low  $d$  there is a point beyond which  $T_c$  vanishes extremely rapidly while  $d$  changes very slowly. Below this point it is extremely difficult numerically to try to go to lower  $d$  values for fixed values of  $N$ .

All scaling was done using three lattice sizes:  $N_1$ ,  $N_2 = N_1 + 2$ , and  $N_3 = N_1 + 4$ . For  $N_1 \leq 9$  many

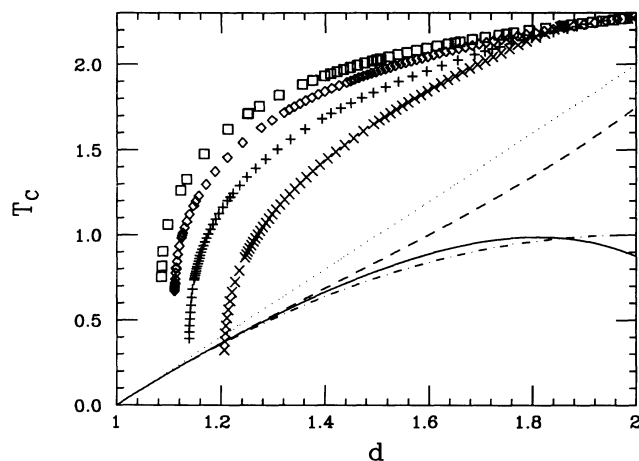


FIG. 3. The critical temperature  $T_c$  is shown as a function of the dimension  $d$ . The plotting symbols have the same interpretations as in Fig. 2. The lines are results of the  $d = 1 + \epsilon$  expansions for the near-planar interface model to the order of one-loop (dotted line) and two-loops (dot-dash line) from Ref. 10, three-loops (dashed line) from Ref. 11, and four-loops (solid line) from Ref. 12. The scale of  $T$  has been chosen so  $J/k_B = 1$ .

different values of  $\nu$  were used. However, for  $N \geq 15$  the construction of the diagonal matrix, using Eqs. (7)–(13), became extremely memory and computer-time intensive (for  $N = 15$  it would take about 3 h of CPU time on a four-processor Cray YMP to obtain a single diagonal matrix). Consequently, for  $N_1 \geq 11$  the only data obtained were with  $\nu = 1$ , for which the construction of the diagonal matrix could be performed by just calculating the energy between states. As opposed to the traditional transfer-matrix method<sup>58</sup> where computer-time and memory limits come from the diagonalization of the matrix, in the present case the limiting part of the calculation is the construction of the diagonal matrix. The numerical diagonalization of the resulting symmetric transfer matrix  $(\underline{D}_H \underline{D}_\nu)^{1/2} \underline{A} (\underline{D}_H \underline{D}_\nu)^{1/2}$  was accomplished using the NAG routine F02FJF on a Cray YMP. Note that the matrix can only be made symmetric in this fashion since all of its elements are non-negative as shown in Sec. II B. The matrix  $\underline{A}$  was broken up into  $N$  sparse matrices formed from a Kronecker product of one matrix  $\underline{a}$  from Eq. (5) and  $(N-1) \ 2 \times 2$  identity matrices. Thus the matrix  $\underline{A}$  never had to be stored in the computation. The critical exponents obtained for each value of  $\nu$  for  $N_1 = 9$  took about 2 h of CPU time on a Cray YMP.

Figure 4 shows the results for the thermal exponent  $y_T$  obtained from Eq. (17) at the finite-size estimate of  $T_c$  obtained by minimizing Eq. (16) and using the symmetrized diagonal matrix in Eq. (9). This is related to the critical exponent  $\nu$  associated with the divergence of the correlation length,  $\xi \sim t^{-\nu}$  near  $T_c$ , since  $\nu = 1/y_T$ .<sup>7,60</sup> Figure 4 shows that the results for  $y_T$  are in excellent agreement with both the  $d = 1 + \epsilon$  expansions<sup>10-12</sup> (particularly near small  $d$  and with the result to third order) and with the results of applying summation methods to

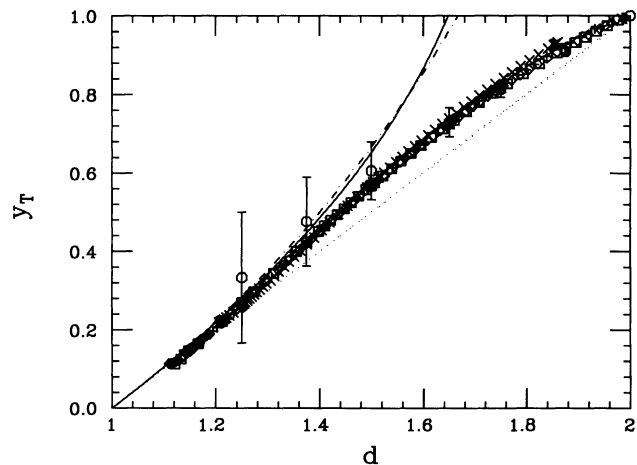


FIG. 4. The value of the thermal critical exponent  $y_T$  is shown as a function of  $d$ . The open circles with error bars are results from resummed  $d = 4 - \epsilon$  expansions from Ref. 9. The other symbols and lines have the same meanings as in Fig. 3. Because of the good agreement between the results, the three-loop  $d = 1 + \epsilon$  expansion results and the data points of the  $d = 4 - \epsilon$  expansion near  $d = 2$  cannot be clearly seen in this figure.

$d = 4 - \epsilon$  expansions.<sup>9</sup> In fact, the agreement between the data from the finite-size-scaling results of the interpolation scheme and the results of both the three-loop  $d = 1 + \epsilon$  expansion and the  $d = 4 - \epsilon$  expansion near

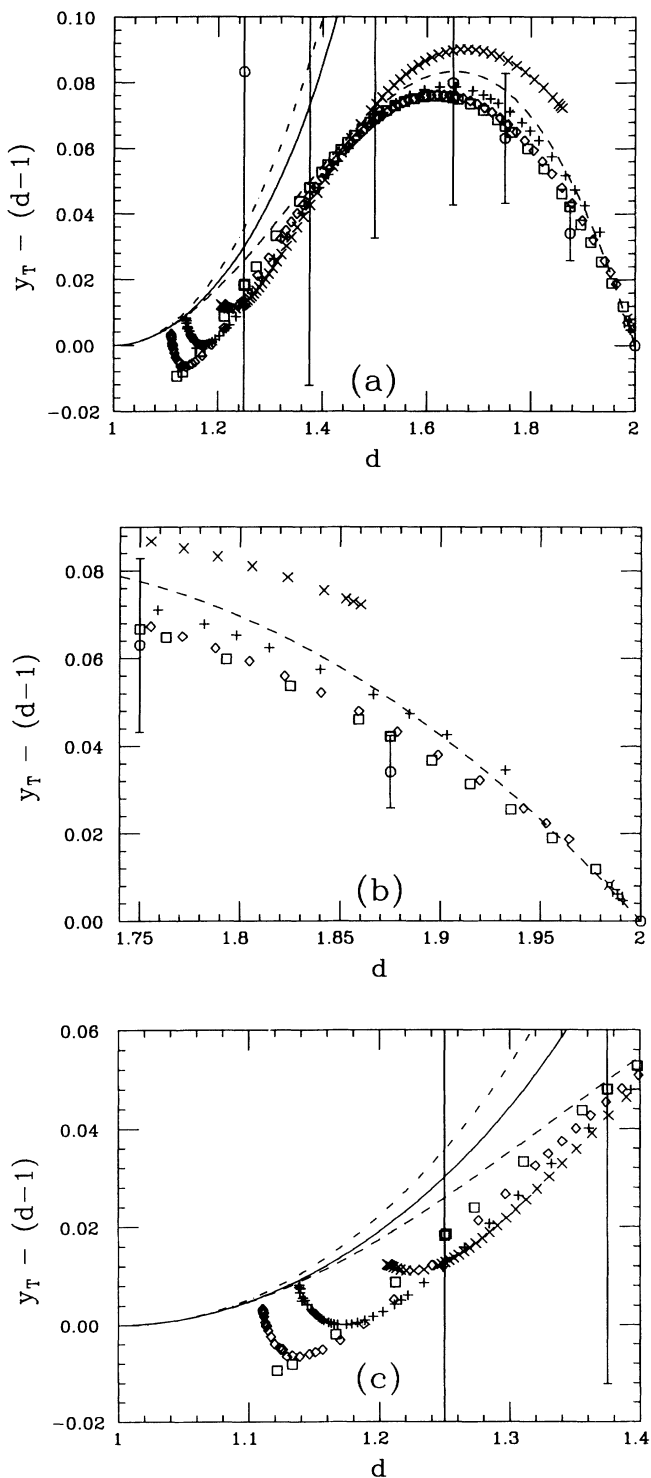


FIG. 5. The thermal exponent  $y_T$  with the  $d = 1 + \epsilon$  expansion to first order subtracted is shown as a function of  $d$ . This shows the finite-size effects in  $y_T$ , which are particularly evident near integer  $d$  as shown in (b) and (c). The plotting symbols and lines have the same interpretations as in Fig. 4.

$d = 2$  is so good it is difficult in Fig. 4 to see the differences between them.

Figure 5 shows  $y_T$  as a function of  $d$  with the lowest-order  $d = 1 + \epsilon$  expansion subtracted. Now it is possible to see the finite-size effects. When  $N_1 = 3$ , the results are not in agreement with the  $d = 4 - \epsilon$  results for  $d$  near 2. However, as  $N_1$  becomes larger the results all agree within the error estimates for  $y_T$  from the  $d = 4 - \epsilon$  results. Also note that the results for  $N_1 = 3$  only give values with  $d \leq 1.86$ , since this is the value obtained when  $\nu = 1$ . As  $N_1$  increases, the value of  $d$  obtained from scaling when  $\nu = 1$  approaches  $d = 2$  as seen in Fig. 5(b). Figure 5(b) is the first time the data with  $N_1 > 9$  (near  $d = 2$ ) can be clearly seen. It is possible to use the data for  $\nu = 1$  in Figs. 4 and 5(b) to obtain derivatives for  $y_T$  with respect to  $d$  evaluated at  $d = 2$ . In this case, the  $\nu = 1$  square-lattice Ising-model exact results<sup>61</sup> can be used for the correlation length as a function of  $N$ . Using these exact results and lattices up to size  $N_1 = 1001$  gives  $dy_T/dd|_{d=2} = 0.46210 \pm 0.00001$ . It is possible to calculate in a similar fashion higher derivatives of  $y_T$  with respect to  $d$  at  $d = 2$ , but this will be left for a future publication.<sup>62</sup> Figure 5(a) shows that the numerical transfer-matrix results agree with the  $d = 1 + \epsilon$  expansion to third order for  $1.35 < d < 1.5$ . However this may be fortuitous since perhaps the  $d = 1 + \epsilon$  expansion is not very good for this large value of  $\epsilon$ . Figure 5(c) shows that although the general trends of the numerical transfer-matrix data and the  $d = 1 + \epsilon$  results are in good agreement, they differ by a value of about 0.01 when  $d \leq 1.3$ . Figure 5(c) also shows that the finite-size effects become extremely large at low dimensions; in fact for the temperatures which could be studied numerically low values of  $d$  can only be obtained for large system sizes. The upturn in the points at small  $d$  seems also to be a finite-size effect, since it moves to lower  $d$  as  $N_1$  becomes larger. Consequently, the study of smaller values of  $d$  would require the use of much larger values of  $N_1$

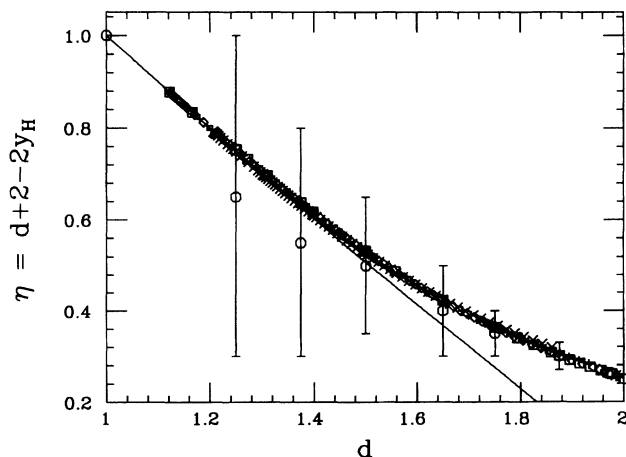


FIG. 6. The exponent  $\eta$  is shown as a function of  $d$ . The plotting symbols have the same interpretations as in Fig. 4. The solid line is obtained from the result for the droplet model, Eq. (3) (Ref. 13).

than are studied here. It is also interesting to note that the most severe finite-size effects, i.e., near the upturn of  $y_T - (d - 1)$  at low  $d$  in Fig. 5, occur near the value of  $d$  where the function  $d = f(v, N_1)$  shown in Fig. 2 changes

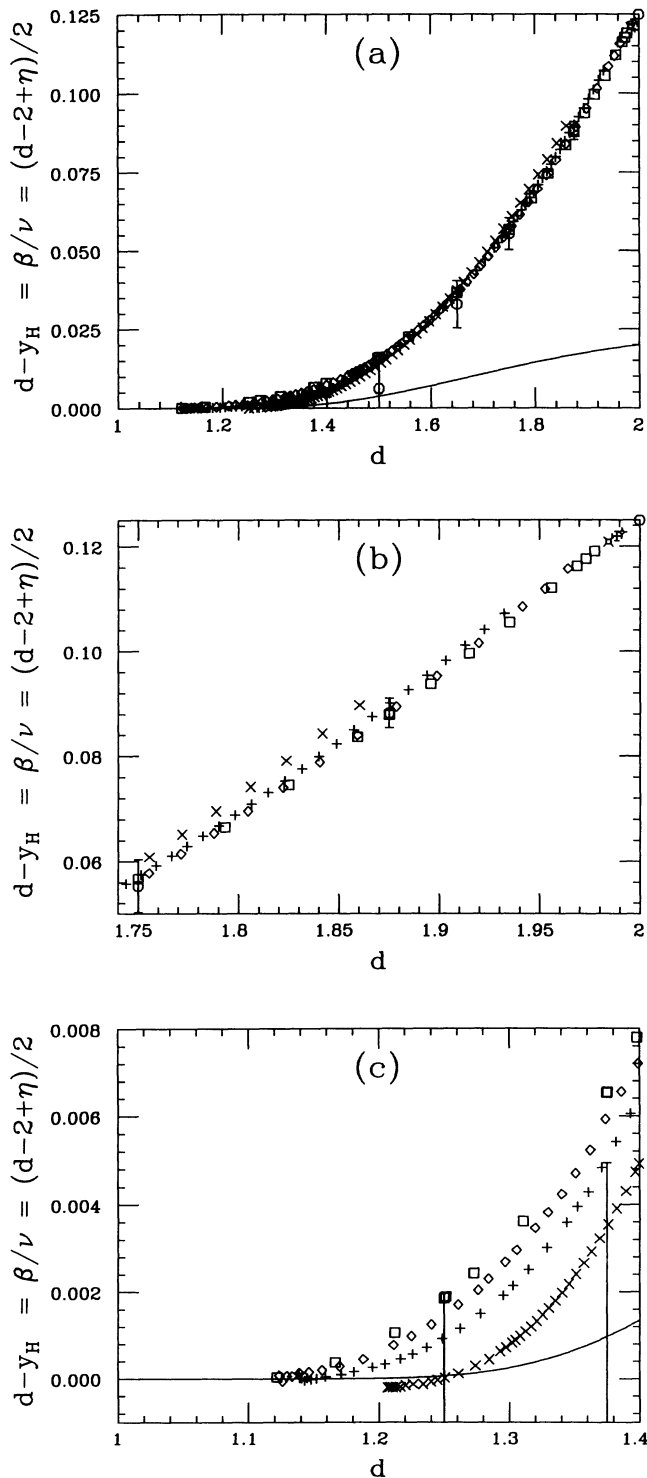


FIG. 7. The exponent  $y_H$  subtracted from  $d$  is shown as a function of  $d$ . The plotting symbols and line have the same interpretations as in Fig. 6. Finite-size effects are illustrated near  $d = 2$  in (b) and near  $d = 1$  in (c).

from falling rapidly to being rather flat.

Figure 6 shows the results obtained for  $\eta = d + 2 - 2y_H$  from Eq. (18) as a function of  $d$  for the symmetric diagonal matrix of Eq. (9). The solid line in the figure is from the droplet model, Eq. (3), with which the data agree at low  $d$ . The transfer-matrix results also agree with the  $d = 4 - \epsilon$  results and the exact value  $\eta = \frac{1}{4}$  at  $d = 2$ . Again the finite-size effects are difficult to see in Fig. 6. Figure 7 shows  $d - y_H$ , with Fig. 7(b) showing the finite-size effects near  $d = 2$  and Fig. 7(c) showing finite-size effects at low  $d$ . Figure 7(b) shows that the results only agree with the  $d = 4 - \epsilon$  result when  $N_1 > 3$ , and there is a small systematic shift between the  $N_1 = 5$  result and the results with larger  $N_1$ . For a given value of  $N_1$  the data point with the largest value of  $d$  in Fig. 7(b) is obtained when  $v = 1$ , and hence gets closer to  $d = 2$  as  $N_1$  increases. For lattice sizes with  $N_1 \leq 15$  one obtains from numerical differentiation that  $dy_H/dd|_{d=2} = 0.73 \pm 0.01$ . Better bounds on this derivative can be obtained by using larger  $N_1$  values, which will be treated in a future publication.<sup>62</sup> Figure 7(c) shows that results fall outside the error bars of the  $d = 4 - \epsilon$  expansion at  $d = 1.375$ , although the errors on data points of the  $d = 4 - \epsilon$  expansion at low  $d$  are extremely large (see Table I). Also, there are again large finite-size effects at low  $d$ . This should not be surprising since the finite systems are trying to mimic a function that has an essential singularity at  $d = 1$ .

Table II gives the numerical transfer-matrix results for  $y_T$  and  $y_H$  obtained at the values of  $d$  where there are series estimates (see Table I) from the resummed Wilson-Fisher expansions in  $d = 4 - \epsilon$ ,<sup>9</sup> and from recent results of a variational method derived from high-temperature series expansions.<sup>48</sup> As seen from the tables and from Figs. 5 and 7 the numerical transfer-matrix results generally agree with the  $d = 4 - \epsilon$  results, except for  $y_H$  at  $d = 1.375$ . The agreement is not as good with the results from Ref. 48. Although the general trend is correct, the transfer-matrix results fall outside of the error estimates in Ref. 48 for  $y_T$  at  $d = 1.875$ , and for  $y_H$  when  $1.5 \leq d \leq 1.875$ . However, the authors in Ref. 48 have difficulty locating  $T_c$  and need to keep  $H$  finite in their study. This may be the source of the difference between the present results and the results of Ref. 48.

Also shown in Table II are results at the dimension  $d = \ln 3 / \ln 2 = 1.585 \dots$ . This dimension was chosen since it is the easiest dimension below  $d = 2$  for which Migdal-Kadanoff bond moving can be employed. The values obtained from the Migdal-Kadanoff bond moving are<sup>15</sup>  $y_T = 0.6302$  and  $y_H = 1.5610$ . These results are near those given in Table II. However, as  $N_1$  becomes larger the value of  $y_T$  appears to converge to a value about 5% higher than the Migdal-Kadanoff result, and the value for  $y_H$  converges to a value about 0.2% higher than the Migdal-Kadanoff result. This agreement is quite good when one considers that the Migdal-Kadanoff result is the exact result for a non-translationally-invariant fractal with a Hausdorff dimension  $d = \ln 3 / \ln 2$ . Differences at other values of  $d$  between the critical exponents from  $d = 4 - \epsilon$  series results and Migdal-Kadanoff results have previously been reported (see Fig. 5 of Ref. 31).

The error estimates in Table II for  $y_T$  and  $y_H$  come from a variety of sources. One error is in the location of  $T_c$  when finding the minimum of  $R(T)$  in Eq. (16) (Fig. 1);  $T_c$  was typically located to about one part in  $10^6$ . Another source of error is that at the finite-size estimate of  $T_c$  the finite-size estimate of  $d$  given by Eq. (15) uses only two system sizes, whereas three system sizes were used to calculate  $T_c$ . An error estimate for  $d$  was obtained by using all three pairs drawn from the three system sizes, and choosing the error to be the difference between the largest and smallest of the three values of  $d$ . This error is largest for small values of  $N_1$ . Additional errors come from the numerical differentiation of Eq. (17) or Eq. (18). These errors were added to the errors obtained by using all pairs drawn from the three values of  $N$ , as was done for error estimates for  $d$ . It is important to realize that all of these error estimates could in principle be reduced further for a given value of  $N_1$ . (The exception is the systematic error due to taking all pairs of the three lattice sizes, which can only be reduced by taking larger values of  $N_1$ .) However, since the error estimates here are comparable to the finite-size effects evident in Table II as  $N_1$  increases, no further work on decreasing the errors was done. The error estimates in Table II should also be used as a guide to the errors

TABLE II. The critical exponents  $y_T$  and  $y_H$  obtained from finite-size scaling of numerical transfer-matrix data using the symmetrized diagonal matrix of Eq. (9) are tabulated for the same values of  $d$  as in Table I. The three system sizes used in the finite-size scaling are  $N_1$ ,  $N_2=N_1+2$ , and  $N_3=N_1+4$ . See the text for a description of the error estimates.

$d$	$N_1$	$y_T$	$y_H$
1.875	5	0.9247 ± 0.0042	1.7852 ± 0.0011
1.875	7	0.9191 ± 0.0008	1.7865 ± 0.0006
1.875	9	0.9171 ± 0.0002	1.7871 ± 0.0001
1.75	3	0.8372 ± 0.0128	1.6905 ± 0.0021
1.75	5	0.8222 ± 0.0035	1.6929 ± 0.0008
1.75	7	0.8180 ± 0.0003	1.6934 ± 0.0004
1.75	9	0.8167 ± 0.0007	1.6934 ± 0.0001
1.65	3	0.7399 ± 0.0124	1.6127 ± 0.0013
1.65	5	0.7288 ± 0.0040	1.6136 ± 0.0004
1.65	7	0.7260 ± 0.0007	1.6136 ± 0.0001
1.65	9	0.7253 ± 0.0004	1.6134 ± 0.0003
1.585...	3	0.6705 ± 0.0122	1.5594 ± 0.0009
1.585...	5	0.6623 ± 0.0048	1.5593 ± 0.0005
1.585...	7	0.6605 ± 0.0012	1.5589 ± 0.0004
1.585...	9	0.6604 ± 0.0005	1.5586 ± 0.0004
1.5	3	0.5728 ± 0.0125	1.4862 ± 0.0002
1.5	5	0.5686 ± 0.0060	1.4852 ± 0.0005
1.5	7	0.5683 ± 0.0022	1.4845 ± 0.0007
1.5	9	0.5691 ± 0.0008	1.4840 ± 0.0004
1.375	3	0.4174 ± 0.0105	1.3715 ± 0.0009
1.375	5	0.4186 ± 0.0075	1.3700 ± 0.0008
1.375	7	0.4206 ± 0.0036	1.3691 ± 0.0008
1.375	9	0.4230 ± 0.0019	1.3685 ± 0.0009
1.25	3	0.2627 ± 0.0004	1.2500 ± 0.0005
1.25	5	0.2622 ± 0.0058	1.2491 ± 0.0004
1.25	7	0.2647 ± 0.0043	1.2485 ± 0.0003
1.25	9	0.2682 ± 0.0033	1.2481 ± 0.0003

on the numerical transfer-matrix data results for  $y_T$  and  $y_H$  in various regions of  $d$  in Figs. 4–9.

Figure 8 presents the result for the critical exponent  $\beta$  associated with the order parameter at  $H = 0$  and  $T = T_c$

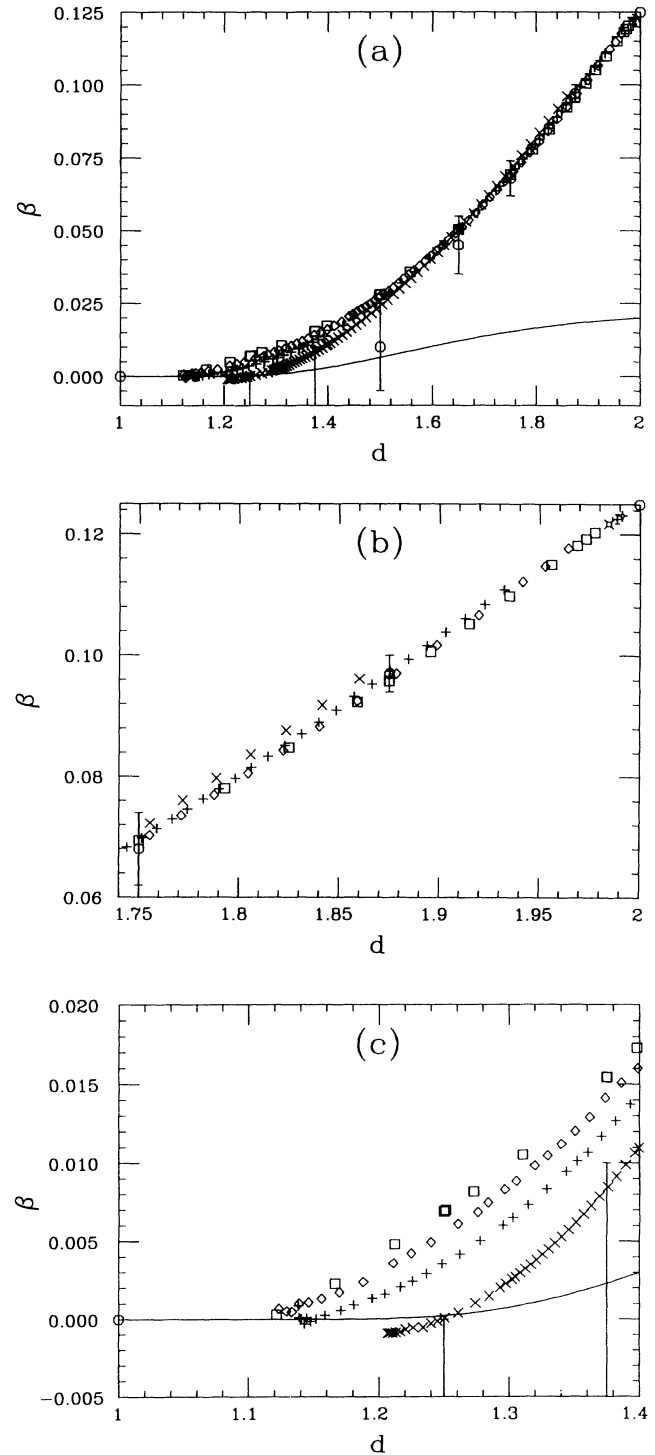


FIG. 8. The exponent  $\beta$  is shown as a function of  $d$ . The plotting symbols have the same interpretations as in Fig. 4. The solid line is obtained from the result for the droplet model [Eq. (3)] and the value for  $y_T$  from the near-planar interface model to three-loop order from Eq. (2). Finite-size effects are illustrated near  $d = 2$  in (b) and at low  $d$  in (c).

where  $O \sim t^\beta$ . The value of  $\beta$  is given by the relation  $\beta = (d - y_H)/y_T$ .<sup>7</sup> Also note that the general trend for  $\beta$  agrees with the results of  $\epsilon$  expansions [Fig. 8(a)], and agrees very well with the  $d = 4 - \epsilon$  expansion at high  $d$  [Fig. 8(b)]. However at low  $d$ , Fig. 8(c), the results are not in very good agreement with the  $\epsilon$  expansion results. Note, however, that the error estimates for the  $d = 4 - \epsilon$  expansion become extremely large at small  $d$ , and in fact at  $d = 1.25$  the physical values  $\beta > 0$  are outside the error estimates. Also, the way  $\beta$  increases as a function of  $d$  is much faster than predicted by the lowest-order term from the droplet model.<sup>13</sup> Note, however, that the droplet-model results grow too slowly, and are far below the exact value  $\beta = \frac{1}{8}$  at  $d = 2$ . For a fixed  $N_1$ , Fig. 8(c) shows that finite-size effects limit the value of  $d$  to which interpolation can be used. Consequently, testing Eq. (3) at lower values of  $d$  would require the use of much larger values of  $N_1$ .

Figure 9(a) shows the exponent  $\gamma$  associated with the order-parameter susceptibility  $\chi$  as a function of  $d$ . At  $H = 0$  near  $T_c$ ,  $\chi \sim t^{-\gamma}$ , with  $\gamma$  obtained from the scaling relation  $\gamma = (2y_H - d)/y_T$ .<sup>7</sup> Again we observe that the

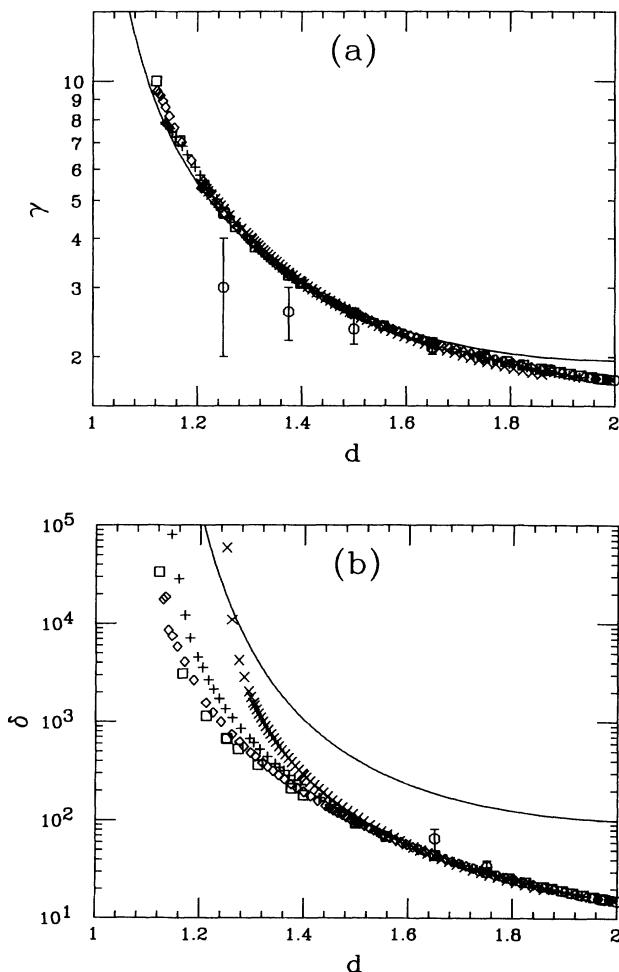


FIG. 9. The critical exponents  $\gamma$  (a) and  $\delta$  (b) are shown as a function of  $d$ . The plotting symbols and line have the same interpretations as in Fig. 8.

general trend for the exponents is correct, and the agreement with the  $d = 4 - \epsilon$  expansion is good only near  $d = 2$ . The agreement with the droplet model results are good to about 10% at low  $d$ . It is also interesting to note that the results from Migdal-Kadanoff bond moving at  $d = 1.585 \dots$ , which yields  $\gamma = 2.439$ ,<sup>15</sup> are very close to the numerical transfer-matrix results.

Figure 9(b) shows the exponent  $\delta$ , which governs the vanishing of the order parameter at  $T_c$  for small  $H$  by  $O \sim H^{1/\delta}$ . The exponent  $\delta$  is given by  $\delta = y_H/(d - y_H)$ .<sup>7</sup> Again there is good agreement with  $d = 4 - \epsilon$  expansion results at high  $d$ , while the  $d = 4 - \epsilon$  results predict unphysical values for  $d = 1.50$ . The results from Migdal-Kadanoff bond moving at  $d = 1.585 \dots$  yield  $\delta = 65.2$ ,<sup>15</sup> which is very close to the numerical transfer-matrix results. However, there is not good quantitative agreement between the  $d = 1 + \epsilon$  expansion results and the numerical transfer-matrix results at low  $d$ .

Another question that must be addressed is how large the differences are between using the symmetric interpolation scheme used above with the diagonal matrix from Eq. (9) and the unsymmetrized scheme with the diagonal matrix in Eq. (7). Figure 10 shows that the function  $d(\nu)$  falls much faster for the unsymmetrized case than for the symmetrized case. One effect of this is that it gives larger errors for  $y_T$  and  $y_H$  in the unsymmetrized case, since the errors are calculated using two system sizes at a time as described above. Note that when  $\nu = 1$  ( $\nu = 0$ ) both

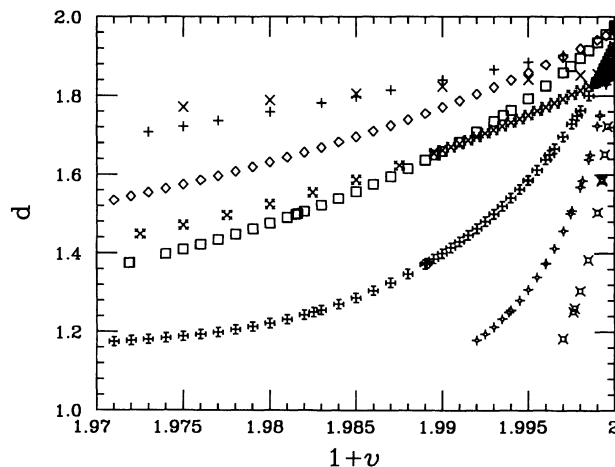


FIG. 10. The value of the dimension  $d$  obtained from scaling is shown as a function of the interpolation parameter  $1 + \nu$ . This illustrates one of the differences between using the symmetrized diagonal matrix in Eq. (9) and using the unsymmetrized diagonal matrix in Eq. (7). The symbols represent results obtained from finite-size scaling of numerical transfer-matrix data from the symmetrized diagonal matrix [Eq. (9)] using three system sizes:  $\times$  for  $N = 3, 5$ , and  $7$ ;  $+$  for  $N = 5, 7$ , and  $9$ ;  $\diamond$  for  $N = 7, 9$ , and  $11$ ;  $\square$  for  $N = 9, 11$ , and  $13$ . The other symbols represent results obtained using the unsymmetrized diagonal matrix [Eq. (7)] using three system sizes: a fancy diagonal cross for  $N = 3, 5$ , and  $7$ ; a fancy horizontal cross for  $N = 5, 7$ , and  $9$ ; a fancy diamond for  $N = 7, 9$ , and  $11$ ; and a fancy square for  $N = 9, 11$ , and  $13$ .

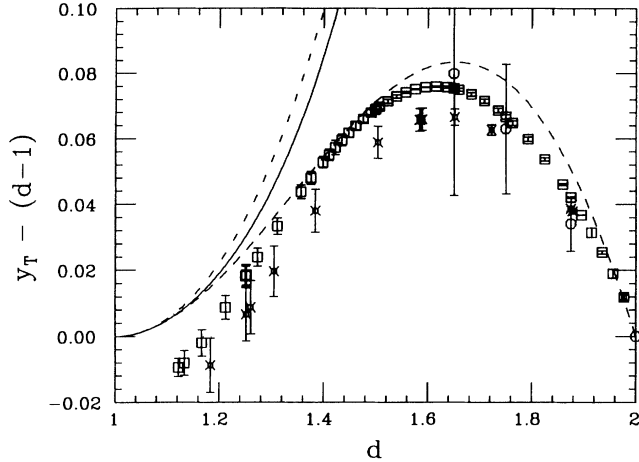


FIG. 11. The thermal critical exponent,  $y_T$ , is shown with the lowest-order results from the  $d = 1 + \epsilon$  expansion subtracted. Only results using system sizes  $N = 9, 11,$  and  $13$  are shown. This illustrates the differences in the critical exponent  $y_T$  between using the symmetrized diagonal matrix in Eq. (9) ( $\square$ ) and the unsymmetrized diagonal matrix in Eq. (7) (fancy squares). The open circles with error bars are results from  $d = 4 - \epsilon$  expansions from Ref. 9. The lines have the same interpretations as in Fig. 3.

the symmetrized and the unsymmetrized versions are the standard  $d = 2$  ( $d = 1$ ) Ising model, and consequently give the same exponents. At other values of  $\nu$  the values for the exponents are different. For the exponent  $y_H$ , it was found that the values from the symmetrized and the unsymmetrized versions agreed to within the error estimates for a given value of  $N_1$ . The same is not true for the exponent  $y_T$ . Figure 11 shows how the exponent  $y_T$  is affected by using the symmetrized or the unsymmetrized diagonal matrix. The general trend in the critical exponents is found to be as expected. However, there are slight differences, as can be seen in Fig. 11. The finite-size effects at low  $d$  set in sooner in the unsymmetrized case than in the symmetrized case. Also in the unsymmetrized case, the convergence as  $N_1$  is made larger appears to be to a value of  $y_T$  that is about 0.01 lower than in the symmetrized case when  $1.3 \leq d \leq 1.75$ . There are two possibilities that could explain this difference. One is that the exponents obtained do depend on the spatial symmetries included in the model, or another that the finite-size effects are much larger than anticipated (and may not be monotonic), and the critical exponents really will converge to the same value as  $N_1$  is made arbitrarily large. It is not possible to decide between these two possibilities with the present system sizes.

#### IV. DISCUSSION AND CONCLUSION

An interpolation scheme that allows one to perform a numerical study of a translationally invariant Ising model between one and two dimensions has been presented. This has been done by finding an interpolation parameter

that continuously changes the connectivity of the lattice, and gives the normal hypercubic lattices when  $d = 1$  or  $d = 2$ . By implementing a finite-size scaling of numerical transfer-matrix data using three system sizes, the critical temperature  $T_c$  and estimates for the finite-size dimension  $d$  as well as results for the critical exponents  $y_T$  and  $y_H$  have been obtained. Other critical exponents are obtained by the use of scaling and hyperscaling relations. The results for the critical exponents are in good agreement with resummed series in  $d = 4 - \epsilon$  dimensions.<sup>9</sup> The results are also in reasonable agreement at low  $d$  with asymptotic results from the near-planar interface model<sup>10-12</sup> and the droplet model.<sup>13</sup> The results also agree at low  $d$  with a recent variational method derived from high-temperature series expansions,<sup>48</sup> but are outside the error estimates of that work for  $y_T$  at  $d = 1.875$  and for  $y_H$  when  $d \geq 1.5$ .

The agreement between the present results and the resummed  $d = 4 - \epsilon$  results also provides further evidence that the results from Ref. 9 at  $d = 3$  may be accurate. These results are within the error estimates from previous Monte Carlo renormalization-group studies<sup>63-65</sup> and in agreement with numerical transfer-matrix results for  $d = 3$ .<sup>46,66</sup> However, these results are in disagreement with very recent extensive Monte Carlo<sup>67</sup> and Monte Carlo renormalization-group studies.<sup>68</sup>

The interpolation scheme presented here can easily be generalized to other lattice models, such as the Potts model. In fact it would be interesting to perform studies to test the theoretical estimates for the  $q$ -state Potts model,<sup>16,69,70</sup> and the  $O(n)$  Heisenberg model.<sup>21</sup>

By inserting interpolated lattices in place of any linear chains in a lattice, it should be possible to study models in dimensions greater than 2. Once such an insertion has been done, the system could be studied using Monte Carlo techniques (since all Boltzmann weights in the interpolated system are positive), and may even be amenable to Monte Carlo renormalization-group studies.<sup>71</sup> It may be possible to utilize this method to study systems with quenched randomness, which could then be compared with theoretical estimates.<sup>19</sup>

The weaknesses of the method presented in this paper should also be kept in mind. One question is whether the thermodynamic limit exists for the interpolation scheme presented here; the possible lack of the existence of this limit is hinted at in Figs. 2 and 3. There is also the question of whether the Ising model in noninteger dimensions has a well-defined field-theory analogue<sup>72</sup> and whether the interpolated model has convexity violations.<sup>73</sup> Another weakness is the lack of a single value of  $\nu$  for a given  $N$  such that the lattice system would have a particular noninteger dimension. However, it may be possible to overcome some of these difficulties. In particular, the interpolation parameter used in this paper is  $f(\nu) = \nu$ , see Eq. (7). However, any function which satisfies  $f(0) = 0$  and  $f(1) = 1$  could have been chosen, which would lead to the dimension as a function of  $\nu$  given by  $d(f(\nu))$ . Thus  $f(\nu)$  could have been chosen to make  $d(\nu)$  have a less singular behavior than  $d(\nu)$  does here. And it may be possible to find a function or functions  $f(\nu)$  for which the thermodynamic limit exists.

## ACKNOWLEDGMENTS

This research was supported in part by the Florida State University Supercomputer Computations Research Institute, which is partially funded through Contract No. DE-FC05-85ER25000 by the U.S. Department of Energy.

Computer time was supplied by Florida State University on their Cray YMP4/32 supercomputer. The author wishes to thank A. Aharony, A. J. Liu, V. Privman, P. A. Rikvold, B. Schmittmann, and R. K. P. Zia for useful discussions.

- <sup>1</sup>M. E. Fisher and D. S. Gaunt, *Phys. Rev. A* **133**, 224 (1964).
- <sup>2</sup>R. Abe, *Prog. Theor. Phys.* **47**, 62 (1972).
- <sup>3</sup>G. A. Baker, Jr. and L. P. Benofy, *J. Stat. Phys.* **29**, 699 (1982).
- <sup>4</sup>K. G. Wilson and M. E. Fisher, *Phys. Rev. Lett.* **28**, 240 (1972).
- <sup>5</sup>E. Brezin, J. C. Le Guillou, J. Zinn-Justin, and B. G. Nickel, *Phys. Lett.* **44A**, 227 (1973).
- <sup>6</sup>D. J. Wallace, in *Phase Transitions and Critical Phenomena*, edited by C. Domb and M. S. Green (Academic, London, 1976), Vol. 6.
- <sup>7</sup>S.-K. Ma, *Modern Theory of Critical Phenomena* (Benjamin, Reading, MA, 1976).
- <sup>8</sup>S. G. Gorishny, S. A. Larkin, and F. V. Tkachov, *Phys. Lett.* **101A**, 120 (1984).
- <sup>9</sup>J. C. Le Guillou and J. Zinn-Justin, *J. Phys. (Paris)* **48**, 19 (1987).
- <sup>10</sup>D. J. Wallace and R. K. P. Zia, *Phys. Rev. Lett.* **43**, 808 (1979).
- <sup>11</sup>D. Forster and A. Gabriunas, *Phys. Rev. A* **23**, 2627 (1981).
- <sup>12</sup>D. Forster and A. Gabriunas, *Phys. Rev. A* **24**, 598 (1981).
- <sup>13</sup>A. D. Bruce and D. J. Wallace, *Phys. Rev. Lett.* **47**, 1743 (1981).
- <sup>14</sup>L. P. Kadanoff, A. Houghton, and M. C. Yalabik, *J. Stat. Phys.* **14**, 171 (1976).
- <sup>15</sup>S. L. Katz, M. Droz, and J. D. Gunton, *Phys. Rev. B* **15**, 1597 (1977).
- <sup>16</sup>B. Nienhuis, E. K. Riedel, and M. Schick, *Phys. Rev. B* **23**, 6055 (1981).
- <sup>17</sup>A. A. Migdal, *Zh. Eksp. Teor. Fiz.* **69**, 1457 (1975) [*Sov. Phys. JETP* **42**, 743 (1976)].
- <sup>18</sup>L. P. Kadanoff, *Ann. Phys. (N.Y.)* **100**, 359 (1976).
- <sup>19</sup>K. E. Newman and E. K. Riedel, *Phys. Rev. B* **25**, 264 (1982).
- <sup>20</sup>R. B. Stinchcombe, in *Phase Transitions and Critical Phenomena*, edited by C. Domb and J. L. Lebowitz (Academic, London, 1983), Vol. 7.
- <sup>21</sup>J. L. Cardy and H. W. Hamber, *Phys. Rev. Lett.* **45**, 499 (1980).
- <sup>22</sup>Z. Alexandrowicz, *Phys. Rev. Lett.* **53**, 1088 (1984).
- <sup>23</sup>A. B. Harris, S. Kim, and T. C. Lubensky, *Phys. Rev. Lett.* **53**, 743 (1984).
- <sup>24</sup>J. A. Aronovitz and T. C. Lubensky, *Phys. Rev. Lett.* **60**, 2634 (1988).
- <sup>25</sup>A. N. Berker and S. Ostlund, *J. Phys. C* **12**, 4961 (1979).
- <sup>26</sup>S. R. McKay and A. N. Berker, *Phys. Rev. B* **29**, 1315 (1984).
- <sup>27</sup>B. B. Mandelbrot, *The Fractal Geometry of Nature* (Freeman, San Francisco, 1983).
- <sup>28</sup>J. Feder, *Fractals* (Plenum, New York, 1988).
- <sup>29</sup>Y. Gefen, B. B. Mandelbrot, and A. Aharony, *Phys. Rev. Lett.* **45**, 855 (1980).
- <sup>30</sup>D. Dhar, *J. Math. Phys.* **18**, 577 (1977).
- <sup>31</sup>B. Bonnier, Y. Leroyer, and C. Meyers, *Phys. Rev. B* **37**, 5205 (1988).
- <sup>32</sup>W. Jezewski and P. Tomczak, *Physica A* **171**, 209 (1991).
- <sup>33</sup>G. Bhanot, H. Neuberger, and J. A. Shapiro, *Phys. Rev. Lett.* **53**, 2277 (1984); *Phys. Lett.* **165B**, 355 (1985).
- <sup>34</sup>B. Bonnier, Y. Leroyer, and C. Meyers, *J. Phys. (Paris)* **48**, 553 (1987).
- <sup>35</sup>B. Bonnier, Y. Leroyer, and C. Meyers, *Phys. Rev. B* **40**, 8961 (1989).
- <sup>36</sup>U. M. S. Costa, I. Roditi, and E. M. F. Curado, *J. Phys. A* **20**, 6001 (1987).
- <sup>37</sup>Y. Gefen, A. Aharony, Y. Shapir, and B. B. Mandelbrot, *J. Phys. A* **17**, 435 (1984).
- <sup>38</sup>B. Lin and Z. Yang, *J. Phys. A* **19**, L49 (1986).
- <sup>39</sup>L. Mao and Z. Yang, *J. Phys. A* **20**, 1627 (1987).
- <sup>40</sup>Y. Taguchi, *J. Phys. A* **20**, 6611 (1987).
- <sup>41</sup>M. A. Novotny, in *Quantum Monte Carlo Methods in Equilibrium and Nonequilibrium Systems*, edited by M. Suzuki (Springer-Verlag, Berlin, 1986), p. 23.
- <sup>42</sup>M. A. Novotny, *Bull. Am. Phys. Soc.* **36**, 540 (1991).
- <sup>43</sup>M. A. Novotny, *Europhys. Lett.* **17**, 297 (1992); **18**, 92(E) (1992).
- <sup>44</sup>M. A. Novotny, in *Physical Phenomena in High Magnetic Fields*, edited by E. Manousakis, P. Schlottmann, P. Kumar, K. Bedell, and F. Mueller (Addison-Wesley, Reading, MA, 1992), p. 533.
- <sup>45</sup>M. A. Novotny, *J. Appl. Phys.* **67**, 5448 (1990).
- <sup>46</sup>M. A. Novotny, *Nucl. Phys. B (Proc. Suppl.)* **20**, 122 (1991).
- <sup>47</sup>M. A. Novotny, in *Computer Simulation Studies in Condensed Matter Physics III*, edited by D. P. Landau, K. K. Mon, and H.-B. Schüttler (Springer-Verlag, Berlin, in press).
- <sup>48</sup>B. Bonnier and M. Hontebeyrie, *J. Phys. (Paris) I* **1**, 331 (1991).
- <sup>49</sup>D. A. Huse, W. van Saarloos, and J. D. Weeks, *Phys. Rev. B* **32**, 233 (1985).
- <sup>50</sup>B. Schmittmann, *J. Phys. A* **17**, 403 (1984).
- <sup>51</sup>R. K. P. Zia, *J. Phys. A* **19**, 2869 (1986).
- <sup>52</sup>H. A. Kramers and G. H. Montroll, *Phys. Rev.* **60**, 252 (1941).
- <sup>53</sup>W. J. Camp and M. E. Fisher, *Phys. Rev. B* **6**, 946 (1972).
- <sup>54</sup>K. Huang, *Statistical Mechanics* (Wiley, New York, 1963), p. 352.
- <sup>55</sup>M. A. Novotny, *J. Math. Phys.* **29**, 2280 (1988).
- <sup>56</sup>P. Audit, *J. Math. Phys.* **32**, 561 (1991).
- <sup>57</sup>V. Privman, in *Finite Size Scaling and Numerical Simulation of Statistical Systems*, edited by V. Privman (World Scientific, Singapore, 1990).
- <sup>58</sup>M. P. Nightingale, in *Finite Size Scaling and Numerical Simulation of Statistical Systems* (Ref. 57).
- <sup>59</sup>R. R. dos Santos and L. Sneddon, *Phys. Rev. B* **23**, 3541 (1981).
- <sup>60</sup>H. E. Stanley, *Introduction to Phase Transitions and Critical Phenomena* (Oxford University Press, New York, 1971).
- <sup>61</sup>M. N. Barber, in *Phase Transitions and Critical Phenomena*, edited by C. Domb and J. L. Lebowitz (Academic,

- London, 1983), Vol. 8, p. 177.
- <sup>62</sup>M. A. Novotny (unpublished).
- <sup>63</sup>G. S. Pawley, R. H. Swendsen, D. J. Wallace, and K. G. Wilson, *Phys. Rev. B* **29**, 4030 (1982).
- <sup>64</sup>H. W. Blöte, J. de Bruin, A. Compagner, J. H. Croockewit, Y. T. J. C. Fonk, J. R. Heringa, A. Hoogland, and A. L. van Willigen, *Europhys. Lett.* **10**, 105 (1989).
- <sup>65</sup>H. W. Blöte, A. Compagner, J. H. Croockewit, Y. T. J. C. Fonk, J. R. Heringa, A. Hoogland, T. S. Smit, and A. L. van Willigen, *Physica A* **161**, 1 (1989).
- <sup>66</sup>M. A. Novotny (unpublished).
- <sup>67</sup>A. M. Ferrenberg and D. P. Landau, *Phys. Rev. B* **44**, 5081 (1991).
- <sup>68</sup>C. F. Baillie, R. Gupta, K. A. Hawick, and G. S. Pawley, *Phys. Rev. B* **45**, 10 438 (1992).
- <sup>69</sup>B. Schmittmann, *J. Math. Phys. A* **15**, 3571 (1982).
- <sup>70</sup>B. Schmittmann and A. D. Bruce, *J. Math. Phys. A* **18**, 1715 (1985).
- <sup>71</sup>E. P. Mürger and M. A. Novotny, *Phys. Rev. B* **44**, 4314 (1991).
- <sup>72</sup>G. A. Baker, Jr. and J. M. Kincaid, *J. Stat. Phys.* **24**, 469 (1981).
- <sup>73</sup>R. B. Griffiths and P. D. Gujrati, *J. Stat. Phys.* **30**, 563 (1983).